NASA TECHNICAL TRANSLATION NASA TT F-15,894

GENERATION AND HEATING OF PLASMAS THROUGH ABSORPTION OF INTENSIVE LASER BEAMS

W. Bögershausen and R. Vesper

Translation of "Über die Erzeugung und Aufheizung von Plasmen durch Absorption intensiver Laserstrahlen," Spectrochimica Acta, Vol. 24B, pp. 103-116. , 1969

(NASA-TT-F-15894) GENERATION AND HEATING OF PLASMAS THROUGH ABSORPTION OF INTENSIVE LASER BEAMS (Kanner (Leo) Associates) 23 p HC $4.25 CSCL 20I N74-32185
G3/25 Unclas 47664

NATIONAL AERONAUTICS AND SPACE ADMINISTRATION
WASHINGTON, D.C. 20546 SEPTEMBER 1974

STANDARD TITLE PAGE

1. Report No. NASA TT F-15,894	2. Government Accession No.	3. Recipient's Catalog No.
4. Title and Subtitle GENERATION AND HEATING OF PLASMAS THROUGH ABSORPTION OF INTENSIVE LASER BEAMS		5. Report Date September 1974 6. Performing Organization Code
7. Author(s) W. Bögershausen and R. Vesper, Physical-Chemical and Electrochemical Institute, Munich University		8. Performing Organization Report No. 10. Work Unit No.
9. Performing Organization Name and Address Leo Kanner Associates Redwood City, California 94063		11. Contract or Grant No. NASw-2481 13. Type of Report and Period Covered Translation
12. Sponsoring Agency Name and Address National Aeronautics and Space Administration, Washington, D.C. 20546		14. Sponsoring Agency Code

15. Supplementary Notes

Translation of "Über die Erzeugung und Aufjeizung von Plasmen durch Absorption intensiver Laserstrahlen," Spectrochimica Acta, Vol. 24B, pp. 103-116, 1969.

16. Abstract The conditions for producing laser plasmas for spectrochemical analysis are discussed using a simplified model. This model is compared with experimental observations on plasmas generated by focused radiation of lasers operated in the normal non-Q-switched as well as in the Q-switched mode. Several materials have been investigated (C, Al, Fe, Zn, W, and Pb) and measurements of the total amount of material being produced by the laser beam, of the kinetic energies of the plasma particles expanding in vacuum, and of the excitation temperature have been made. In addition, time-resolved observations have been made. Plasmas produced by normal mode laser pulses exhibited excitation temperatures of 4900°K (C) up to 7900°K (W), while those produced by a series of giant pulses had temperatures up to 12,000°K (Fe). In the latter case, average particle energies of about 3.5 eV have been measured under the same conditions.

17. Key Words (Selected by Author(s))	18. Distribution Statement
	Unclassified-Unlimited

19. Security Classif. (of this report)	20. Security Classif. (of this page)	21. No. of Pages	22. Price
Unclassified	Unclassified	21	

GENERATION AND HEATING OF PLASMAS THROUGH ABSORPTION OF INTENSIVE LASER BEAMS

W. Bögershausen and R. Vesper
Physical-Chemical and Electrochemical Institute,
Munich University

1. Introduction

/103*

Interest has been aroused in the idea of using focused laser radiation to generate high-temperature plasmas by vaporizing solids, e.g. in the analysis of emission spectra. Soon after the invention /104 of the ruby laser, Brech [1] employed focused laser radiation to vaporize specimen materials, the resulting vapor being additionally excited through a transverse spark gap. In numerous other works [2-7], the laser excitation was investigated in comparison with conventional spectrochemical methods of analysis. The advantages of this excitation consist in a systematic local analysis and in direct excitation of even non-electrically-conducting specimens. Because of the high optical density of laser plasmas, one must rely on additional aids such as transverse spark excitation of the expanding plasma. This explains the interest in the objective of the present work, namely investigating the properties of plasmas resulting from vaporization of solids by focused laser radiation. The experiments were conducted with relatively low irradiation intensities (a few 10^6 to 10^8 W/cm^2), producing the most effective vaporization of the specimen and heating of the plasma to temperatures at which atomic lines are optimally excited.

The laser radiation consisted both of many statistically distributed relaxation pulses (from now on, called normal pulse mode) and of so-called giant pulses, produced by control of the laser emission by an optical switch in the resonator. For both

---

* Numbers in the margin indicate pagination in the foreign text.

cases, a large number of experimental and theoretical investigations have been conducted on laser plasmas. Normal pulse laser plasmas were investigated by e.g. Ready [8], Harris [9], Honig [10], Howe and Molloy [11], Chang and Birdsall [12] and Neuman [13]. Experimental studies on giant pulse laser plasmas were carried out by e.g. Chang and Birdsall [12], Neumann [13], Ehler [14], Ready [8, 15], Linlor [16], Namba et al. [17], Gregg and Thomas [18, 19], Archbold et al. [20, 21], Opower and Press [22], and Linlor [23]. /105 Giant-pulse laser plasmas were theoretically described by Askaryan and Moroz [24], Dawson [25], Zeldovich and Raizer [26, 27], Krokhin [28, 29] and Engelhardt [30].

2. Estimates on Vaporization of Specimens and Origin of Plasma

The dynamic theory of the origin of plasma in the absorption of intensive laser radiation requires that vaporization and plasma heating be considered simultaneously. The complicated interaction between the two, however, causes great difficulties, so that such a representation was not attempted. On the other hand, considering them separately is justified only in limiting cases. One of these arises with low irradiation intensities, when the absorption of radiation in the resulting plasma can be neglected. The other involves high radiation densities, when most of the incident laser energy is transformed in the plasma. An order-of-magnitude estimate of the limit between the two extreme cases is given by the measurements of the recoil pressure of the vaporizing plasma of Gregg and Thomas [19].

2.1. Vaporization

Estimates on the maximum amount of material which can be vaporized can be obtained from energy balance considerations. With simplifying assumptions on the timewise and spatial characteristics of the focused radiation, the conditions which would

justify neglecting thermal conduction losses at low irradiation densities can be derived [8, 31-32]. Ready [33] has made measurements on the losses, which can be considerable particularly for metals due to reflection of the radiation, in the case of interest here, i.e. low radiation densities. These measurements yielded values of less than 10%. Nevertheless, certain doubts remain with respect to these observations, since the measuring method employed was not capable of distinguishing between the self-compensating action of a high degree of reflection and "hot spots" in the laser beam, i.e. major inhomogeneities in radiation intensity over the cross section of the beam. Therefore, even with lower irradiation densities, handbook values for reflection losses will have to be used in the calculations, whenever they are known for the relevant temperature ranges (see below).

Neglecting all losses, the energy balance reads /106

$$\iiint (Q_v + Q_s + C(T_v - T_0))\rho \, dx \, dy \, dz = \iiint E_a(x, y) \, dx \, dy \, dt \qquad (1)$$

where Q_V, Q_S = enthalpies of vaporization and melting, C = specific heat, T_V = vaporization temperature, T_0 = initial temperature, ρ dx dy dz = amount of material of the specimen vaporized in the time dt (ρ = density), z = direction perpendicular to specimen surface, and $E_a(x,y)$ = energy density of absorbed radiation.

The losses to be considered are accordingly deducted from the right side of equation (1). Expressed as an atomic vaporization rate per element of area dxdy, equation (1) reads

$$\frac{dN(x, y)}{dt} = \frac{LW_a(x, y)}{M(Q_v + Q_s + C(T_v - T_0))} \qquad (2)$$

L = Lodschmidt number, M = molecular weight, W_a = power density of absorbed radiation.

Assuming that all atoms or molecules in the specimen which have absorbed an energy sufficient for vaporization leave the specimen at right angles to the specimen surface with the mean thermal velocity $\bar{u}_{th} = (8\ kT/\pi m)^{1/2}$ (T = vaporization temperature, m = mass of molecules or atoms), a simple relationship is obtained between the vaporization rate and the particle density N' of the resulting vapor

$$\frac{dN}{dt} = \tfrac{1}{4}\bar{u}_{th} \cdot N' \qquad (3)$$

From this is obtained, using the relationship for ideal gases (suppressing the spatial dependence of radiation density over the focal spot):

$$\frac{dN}{dt} = p(2\pi kTm)^{-1/2} \qquad (4)$$

where $p = (dN/dt)m\bar{u}_{th}$ is the vapor pressure of the resulting vapor or the recoil pressure exerted on the specimen by the vaporizing atoms. Letting ε_v and ε_{kin} be the total vaporization energy or kinetic energy in the vapor state, calculated per atom, we obtain [24]:

$$p = Wa(2\pi kTm)^{1/2}(\varepsilon_v + \varepsilon_{kin})^{-1} \qquad (5)$$

Equation (4) is plotted in Fig. 1. The figures used were those given in Honig [34], which were also extrapolated. This greatly simplified model will be discussed in connection with the experimental results.

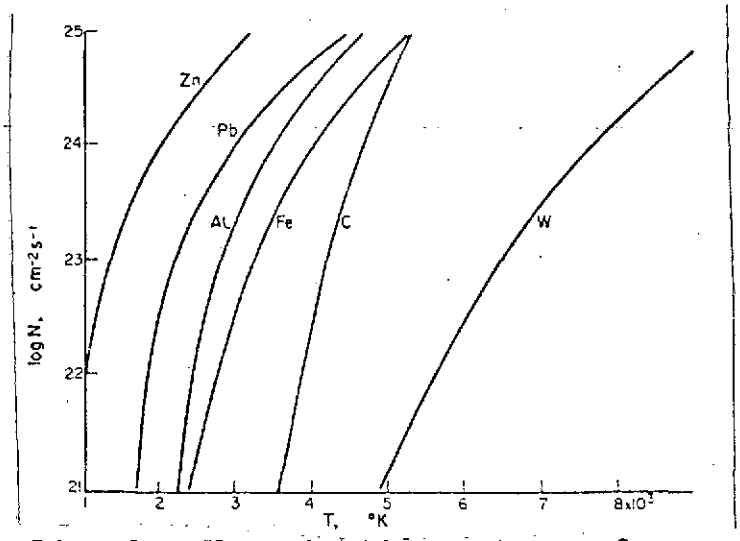

Fig. 1. Vaporization rate as function of surface temperature.

2.2. Absorption of Radiation in the Plasma

While practically relaxation-free transformation of the radiation energy into thermal energy can be presumed in the solid specimen [8], and was confirmed experimentally [33], this can no longer be done directly in the resulting plasma. /107

Because of the steepness of the vapor-pressure curves (Fig. 1), the temperatures of the resulting vapor are not high enough, even with high vaporization rates and thus high absorbed radiation intensities, to ensure a degree of thermal ionization sufficient for effective radiation absorption. Moreover, the field strength F ((V/cm) in the focused laser beam

$$F = 19.4 \cdot W^{1/2} \qquad (6)$$

with W in W/cm^2 are not enough larger than the interatomic field strengths to produce the required degree of ionization. Using the method of Archbold et al. [20] to estimate the plasma heating resulting from the Kramers-Unsöld absorption coefficients [36], with initial plasma temperatures below 10^4°K, and even with irradiation densities of 10^8 W/cm^2 and a typical pulse duration of a few 10^{-7} sec, the temperature increases are only on the order of 100°K, which are very inconsistent with the observations.

Therefore, it appears necessary to assume an initially non-thermal ionization mechanism for the heating of the plasma. When the irradiation densities in the plasma are high, the free

electrons present absorb more radiation energy via elastic collisions than they lose via thermalization collisions and inelastic collision processes with the atoms and ions, so that they reach the ionization energy of the plasma atoms and, by ionization, produce new generations of free electrons. This process of cascade photoionization, which is similar to the Townsend cascade ionization in an electrical field, was investigated by Zeldovich and Raizer [26] for the discharge ionization of cold gases. The cascade-like growth of the electron avalanche due to ionization can be described approximately by /108

$$N_a = N_0 \exp(t/\tau) \qquad (7)$$

N_0, N_a = electron density at outset or after time t, τ = cascade time constant. For effective plasma heating and effective ionization (e.g. simple ionization of the plasma), $t_1 = \tau \ln(N_1/N_0)$ must be less than the duration of the laser pulse. The situation relative to vaporizing the plasma from a solid is more favorable than that in the case treated in [26], since a relatively high initial electron density N_0 can be anticipated.

3. Experimental Setup

The laser employed is of conventional design. Along the focal lines of an elliptical cylinder of electropolished pure aluminum are situated in each case the 2wx 1/4 inch ruby with TIR polishing (1), (see Fig. 2) and the flash lamp. The second resonator mirror is an external dielectric mirror (3) with 70% reflection at 6943 Å. If desired, an optical switch can be inserted in the space between the ruby and the external resonator mirror. In this case, the switch consists of a quartz cuvette filled with kryptocyanin (2), the transmittance of which is chosen in accordance with the desired emission characteristic of the laser. The prism (5) deflects the laser beam toward a glass

lens (focal length f = 25 mm) (6), which focuses the laser beam on the surface of the specimen (7). The focus of the focusing lens is situated on the optical axis of the spectrograph (Q 24, Zeiss-Jena) in the plane of the entry slit. A 1:1 image of the resulting vapor cloud is produced with a quartz lens (8) on the entry slit (9). The spectrum of the vapor cloud is recorded on a high-sensitivity film (Ilford HPS).

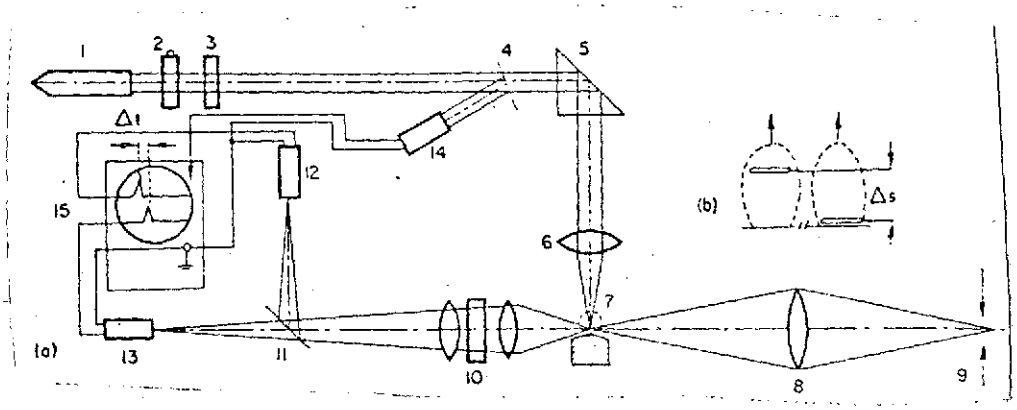

Fig. 2. Setup of experiment for vaporizing and heating specimens by means of laser beams.
1. ruby; 2. Q switch; 3. resonator mirror; 4, 11. beam splitter; 5. deflection prism; 6. focusing lens; 7. specimen; 8. quartz lens; 9. spectrograph slit; 10. imaging lens with interference filter; 12, 13. photomultiplier; 14. photodiode; 15. oscillograph

With the setup in Fig. 2(b) (10÷15), the time behavior of the /109
vapor cloud was also investigated. Here, a magnified image of the laser vapor cloud is produced on the photocathodes of two secondary-electron multipliers (12, 13), the image beam having been split by a beam splitter in a 1:1 ratio to the two multipliers. The photocathodes of the two multipliers are covered by masks with small open slits, so that the image of the expanding laser vapor cloud produces signals with time delays in the two multipliers, depending on the distance of the two slits located at different heights above the image line of the specimen surface and depending on the magnification ratio. By measuring the time differences in

the signals with a two-beam oscillograph, statements can be made on the propagation velocity of the luminous front of the vapor cloud. Furthermore, the signal of each multiplier supplies information on variations in time of the emission behavior of a specific element of volume of the vapor cloud; certain spectral regions can be selected out by interference filters.

The radiation energy emitted by the laser was measured with a calorimeter described in Röss [37], p. 278. The radiation power of a laser pulse was determined by simultaneously recorded the pulse form of the photodiode signal on the oscillograph screen, suitable color filters being placed in front of the photodiode.

The irradiation density focused on the specimen surface was first determined from the optical laws of imagery by measuring the angular divergence of the laser beam. On the other hand, a better method is direct measurement of the diameter of the focal spot. This was done here by measuring holes burned in thin aluminum foil. However, these measurements represent only mean values, and ignore the presence of hot spots in the laser beam. Within the limits of reproducibility, the following laser operating conditions were employed for generating laser plasmas:

3.1. Normal Pulse Mode

With no optical switch, the pulse form depicted in Fig. 3(a) was obtained (the pumping pulse form was that of an aperiodically damped oscillation). At the maximum energy of 1 Wsec, which was employed in most of the experiments, the pulse consists of about 100 individual spikes, each about 0.8-1 µsec long, so that the mean radiation power of a spike is about 10^4 W. The duration of the overall pulse is about 500 µsec. The mean irradiation density in the focus is about $1.5\text{-}2 \cdot 10^7$ W/cm^2, but the individual spikes which occur about 50 to 100 µsec after the beginning of

laser emission have focused irradiation densities of about 5 to $8 \cdot 10^7$ W/cm^2, corresponding to the pumping power. Fig. 3(b) shows the shape of the spike on an enlarged time scale.

3.2. Multiple Pulse

By inserting the optical switch, the laser emission depicted in Fig. 4(a) was obtained when the kryptocyanin concentration was such that the cuvette had a transmittance of about 48% at the laser wavelength. The laser emits about 10 individual pulses over a period of 400-500 sec with a total energy of about 0.35-0.45 Wsec. The shortest time interval between two pulses is more than 10 sec, the pulses at the beginning being closer together because of the power curve of the pumping light source. The average irradiation density of an individual pulse is $2\text{-}3 \cdot 10^8$ W/cm^2. /110
Fig. 4(b) shows an individual pulse of the type described.

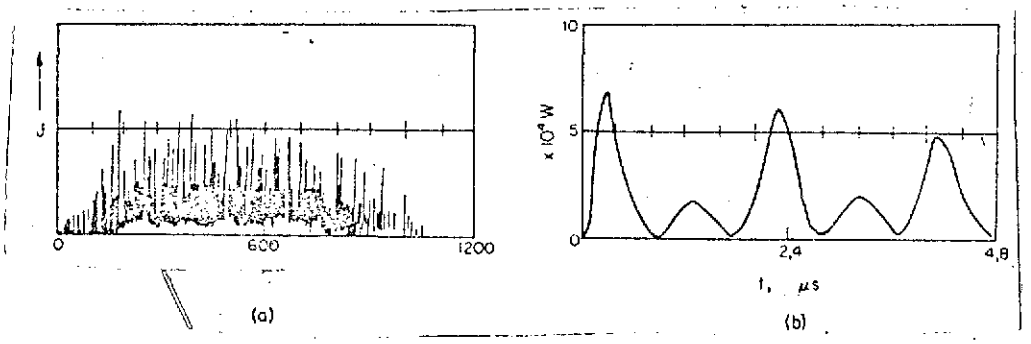

Fig. 3. (a) Pulse form of a laser in "normal mode." (b) Enlarged section (time scale expanded).

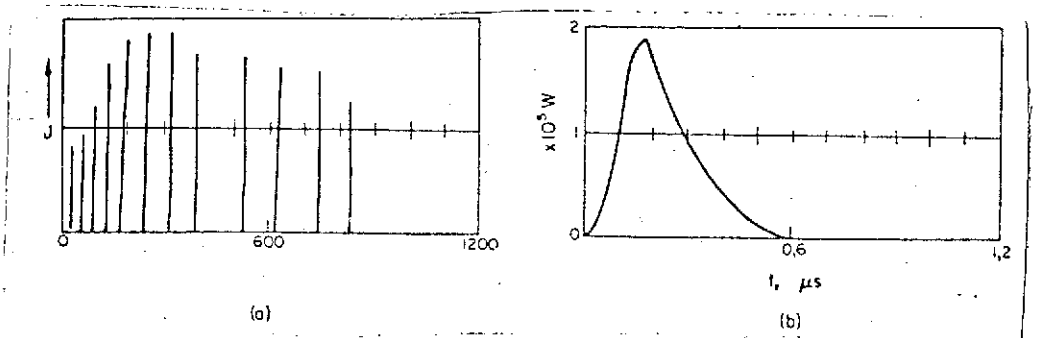

Fig. 4. (a) Laser emission in "multiple-pulse mode." (b) Enlarged section (time scale expanded).

3.3. Giant Pulses

When the kryptocyanin concentration is increased, individual giant pulses are obtained with a duration of 70 nsec (half-power width) and an energy of about 0.03 Wsec. The radiation-power figures may include an error of 20% in the individual measurements.

4. Removal of Material During Vaporization

The detrition per laser firing was determined by measuring the crater volume under an incident-light microscope. However, this should not be uncritically equated with the amount of material escaping from the specimen in the form of vapor. When firing with normal pulses, the well-known scintillation can be seen. As suggested by the appearance of the resulting craters as well, this can be accounted for by liquid material being expelled from the crater by the high recoil pressure during the vaporization. The successive spikes of a normal pulse have widely varying intensities, so that preceding spikes with lower than average radiation powers are just sufficient to heat the specimen above the melting point without substantially vaporizing it. This produces a deep molten zone, which is vaporized by a subsequent spike of higher irradiation density and pushed or flung out by the accompanying recoil pressure. By changing the spike interval (by means of the optical switch), it can be arranged that the specimen temperature drops /111
below the melting point of the material before the next spike arrives, thus avoiding scintillation. With individual pulses, the effect of scintillation cannot appear, since the molten zone has a vanishingly small extent due to the steep temperature gradient. This model is supported by the observation that subliming specimens such as graphite exhibit no scintillation, and by measurements of Neuman [13], who studied the recoil pulses of materials vaporizing under different conditions.

With relatively lower irradiation densities ($< 10^6$ W/cm^2), a boiling lag can also be responsible for scintillation, as shown by observations of Harris [9]. The spray of molten specimen material means that the laser light will be strongly scattered on the drops, and thus will make only a diminished contribution to the vaporization of the specimen.

To estimate the total fraction of laser radiation utilized for vaporization, absorption in the resulting plasma must be taken into account. This can be done by estimating the condition $\kappa_l \cdot l = 1$, assuming complete simple ionization of the plasma. It is assumed that the plasma expands at right angles to the specimen surface with a vaporization rate estimated in accordance with equation (2) and with a speed corresponding to the associated vaporization temperature. This provides a rough approximation for the particle density in calculating the extinction coefficient.

TABLE 1. AMOUNT OF SPECIMEN VAPORIZED. MEASUREMENTS COMPARED WITH VALUES CALCULATED FROM EQUATION (2)

	Lead	Aluminum	Iron	Graphite	Tungsten	Zinc
1	3.30	2.13	1.70	0.85	0.78	$5.25 \cdot 10^{18}$ Atoms
2	1.63	1.09	0.60	0.37	0.15	$2.74 \cdot 10^{18}$ Atoms
3	0.50	0.50	0.35	0.44	0.20	0.52
4	1.17	0.75	0.60	0.30	0.27	$1.84 \cdot 10^{17}$ Atoms
5	2.36	2.45	1.89	1.17	1.37	$2.07 \cdot 10^{16}$ Atoms
6	1.32	—	1.77	3.27	1.51	$1.58 \cdot 10^{16}$ Atoms
7	0.11	—	0.30	1.10	0.50	0.09
8	0.56	—	0.94	2.80	1.10	0.76

In Table 1, the values calculated from equation (2) for specimen vaporization are compared with experimental values obtained from a number of individual measurements. In some of the calculated values (Lines 1 and 4), plasma heating is ignored; in others (Line 5), the plasma resulting from vaporization is assumed to be completely ionized. The average difference between

measurements amounted to about 30%; in each case, the means were taken from a series of 10 measurements.

Line 1 (calculated) and Line 2 (measured) refer to vaporization with normal pulses of 1 Wsec energy and a mean irradiation density of $3 \cdot 10^7$ W/cm^2. Line 3 gives the ratio of the values in Line 2 to those in Line 1. Lines 4 and 5 (calculated) and 6 (measured) apply to giant pulses with an energy of about 0.035 Wsec and a mean irradiation density of $2 \cdot 10^8$ W/cm^2. Lines 7 and 8 give the ratio of the measured values to the calculated ones. In Line 7, only the vaporization energy of the solid is taken into account in the energy balance of equation (1), while in Line 8, the energy balance is calculated under the assumption that a fraction of the radiation energy is expended for complete simple ionization of the plasma. Even though these measurements provide only limited evidence about the overall progress of vaporization and plasma generation, they nevertheless contain certain information. Initially, it should be remarked that the assumption of complete ionization of the plasma results in better agreement between the calculated and measured values. The differences can then be accounted for by the fact that specimens with low boiling point and enthalpy of vaporization and low ionization potential (lead) are ionized at an early stage of the laser pulse, so that still more radiation energy can be used for heating in the plasma. On the other hand, specimens with high enthalpy of vaporization, high boiling point, and high ionization energy (carbon), with the given simplifications, show a difference between theory and experiment opposite to that of lead. In the dynamics of the process, the plasma is obviously not completely ionized, so that the radiation energy is chiefly used for vaporization, because of the low absorption in the plasma.

/112

5. Non-Time-Resolved Measurements of Plasma Temperatures

The details and execution of the temperature measurements for these studies have been described in a previous work [38]. At this point, the results obtained shall the critically analyzed once more. Temperature measurements are based on the assumption of a Boltzmann occupancy of the energy terms. This assumption will be reviewed here in the light of measurements of the excitation temperature (so-called two-line method). For this purpose, the image of the plasma is projected directly onto the spectrograph slit. Even a qualitative consideration of the spectra of laser plasma (see Fig. 5) provides some information on the possibilities and limitations of this method. Directly above the specimen surface, there is a strong continuous spectrum; the lines are very broadened, and to some extent even washed out in the continuous spectrum. Resonance lines for laser plasmas in air (but not in vacuum), exhibit strong self-reversal; Fraunhofer lines of the specimen material appear in the continuous spectrum. With multiple giant pulses, the continuous spectrum has a sharp boundary at a certain height above the specimen surface. In accordance with the views of Raizer [27], this boundary is interpreted as the front of the discharge or cascade ionization wave. The propagation velocity of about $5 \cdot 10^6$ cm/sec, estimated from the height of the continuous spectrum and the duration of the laser pulse, is consistent with the values given by Raizer. These properties of laser plasmas impose certain restrictions on the applicability of the two-line method. For the reasons given above, the line intensities cannot be compared directly above the specimen surface. The measurements were therefore carried out at a height of about 0.5 to 1 mm above the specimen surface.

Measurements were also taken on the continuous spectrum directly above the specimen surface. Absolute calibration of the film material employed was conducted with the aid of black-body /113

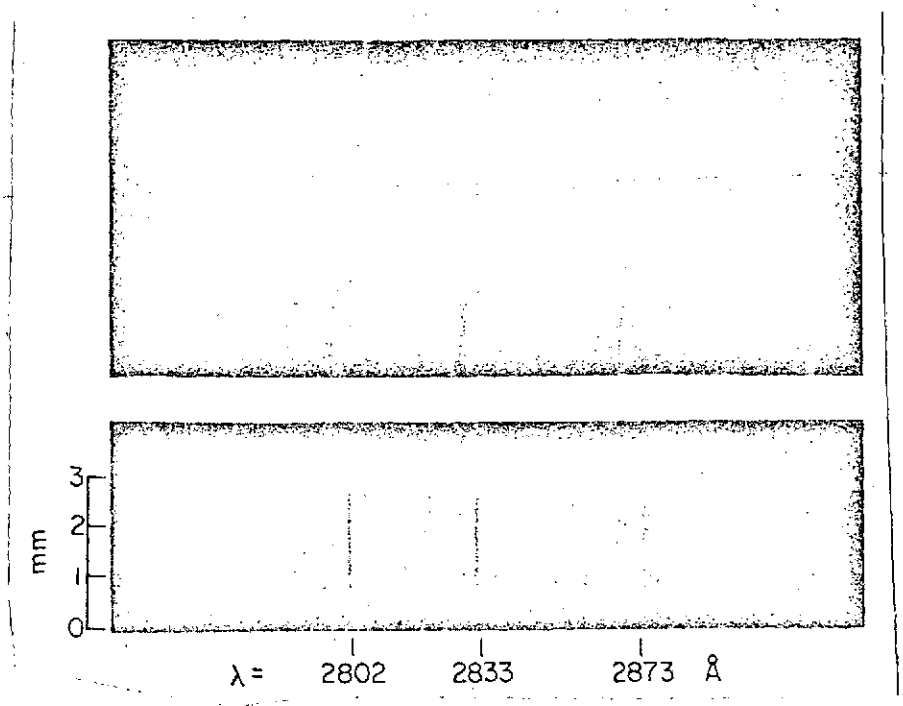

Fig. 5. Section from a lead spectrum. Top: vaporization at 0.5 torr. Bottom: air 1 atm. Multiple giant pulse.

radiation from a carbon arc crater. If the continuous spectrum of the laser plasma (only spectra of giant-pulse laser plasmas were studied) is treated as that of a black body, the very low temperature of about 5000 to 6000°K is obtained, in agreement with the measurements of Archbold et al. [20]. Equally low values are obtained when the measurements are compared with the spectral distribution of the intensity of continuous electron-bremsstrahlung spectra [39]. In this connection, it should also be mentioned that using the zinc triplet lines, which are known to be strongly absorbing, to determine color temperature in giant-pulse laser plasmas in atmospheric air yielded color temperatures above 28,000°K about 0.5 mm above the specimen surface, but only about 10,000°K directly above the specimen surface -- in better agreement with the observations mentioned above. For a summary of the measurements, see [38].

6. Determining Electron Density from Line Width

The electron density in the plasma was also determined, in this case by measuring the width of the 3072 Å zinc line. With the high density of charged particles in the plasma, the quadratic Stark effect is the main cause for the broadening of the lines. The mean field strength F

$$F = 2.6 \cdot e \cdot N^{2/3} \text{ (V/cm)} \qquad (8)$$

given by Debye in terms of the density N of charged particles (e = elementary charge) broadens and shifts the lines. The pure spreading (half-power width) is given by [36]

$$\Delta\nu = (\pi^{4/3}/c) \cdot w^{1/3} \cdot C^{2/3} \cdot N \text{ (cm}^{-1}) \qquad (9)$$

c = velocity of light, u = $(3kT/m)^{1/2}$ is the thermal velocity of the particles, and C is the Stark constant, the value of which was taken from the work of Bardocz et al. [40] (C = $2.371 \cdot 10^{-14}$ $cm^4 sec^{-1}$).

The field strength of the focused laser radiation F = $= 19.4\ W^{1/2}$ (with W in W/cm^2) is superimposed on the coulomb fields of the charged particles. An irradiation density of 10^8 W/cm^2 generates the same field strength as would correspond in the mean to a density of charged particles of $4 \cdot 10^{17}$ cm^{-3} in accordance with equation (8). For the reasons given above, the widths of the lines could not be measured directly above the surface of the specimen. Spectra were measured for plasmas generated by multiple giant pulses (irradiation density about $2 \cdot 10^8$ W/cm^2). At heights of 1.1 and 1.75 mm above the specimen, this gave charged-particle densities of $2.5 \cdot 10^{18}$ cm^{-3} and $1.8 \cdot 10^{18}$ cm^{-3}

respectively for a plasma in atmospheric air. For a plasma expanding in an ambient pressure of 0.5 torr, $N = 2 \cdot 10^{18}$ cm^{-3} was also found 1.1 mm above the specimen. Using the values given by Griem [41] for the Stark effect half-power width of the aluminum line $\lambda = 3944$ Å, the density of charged particles was, as a comparison, determined for an aluminum plasma in atmospheric air generated by normal pulses of about $3 \cdot 10^7$ W/cm^2. $N = 7 \cdot 10^{17}$ cm^{-3} was found 0.4 mm above the specimen surface. /114

7. Time-Resolved Studies

Time-resolved studies of the plasma emission were made with the photomultiplier arrangement described above. The observations are reproduced in some sample oscillograms (Figs. 6 and 7). Fig. 6 shows the emission of a carbon plasma produced by vaporization with normal pulses ($W = 3 \cdot 10^7$ W/cm^2) in air. Directly above the specimen surface, the emission fluctuates widely (Fig. 6a). A laser spike can be assigned to each emission spike. In accordance with the emission characteristic of the laser (Fig. 3a), the development of the plasma does not begin until about 15-20 µsec after the beginning of the laser pulse. The emissions (Fig. 6b) observed higher above the specimen surface (in this case 1.6 mm) exhibit lesser fluctuations -- evidence that expansion and vaporization largely counterbalance each other -- and the development of a well-defined plasma front due to molecule formation (CN) with the surrounding air. If the propagation velocity of this front is /115

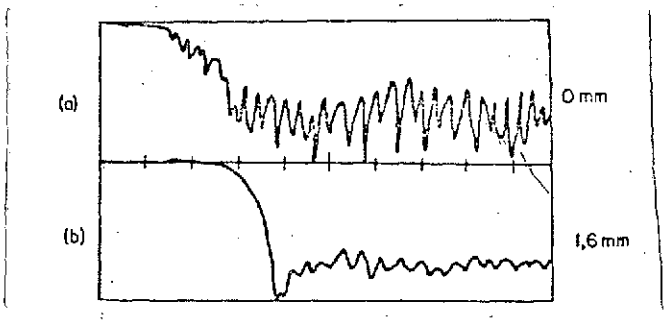

Fig. 6. Emission of a carbon plasma at different heights (a,b) above the specimen. Vaporization by normal pulses in air, 1 kg/cm² (horizontal axis 10 µsec/division). The ordinates represent relative intensity.

measured as in Howe and Molloy [11], a value of $2 \cdot 10^4$ cm/sec is obtained with good consistency. Measurements on other specimen substances yielded similar values.

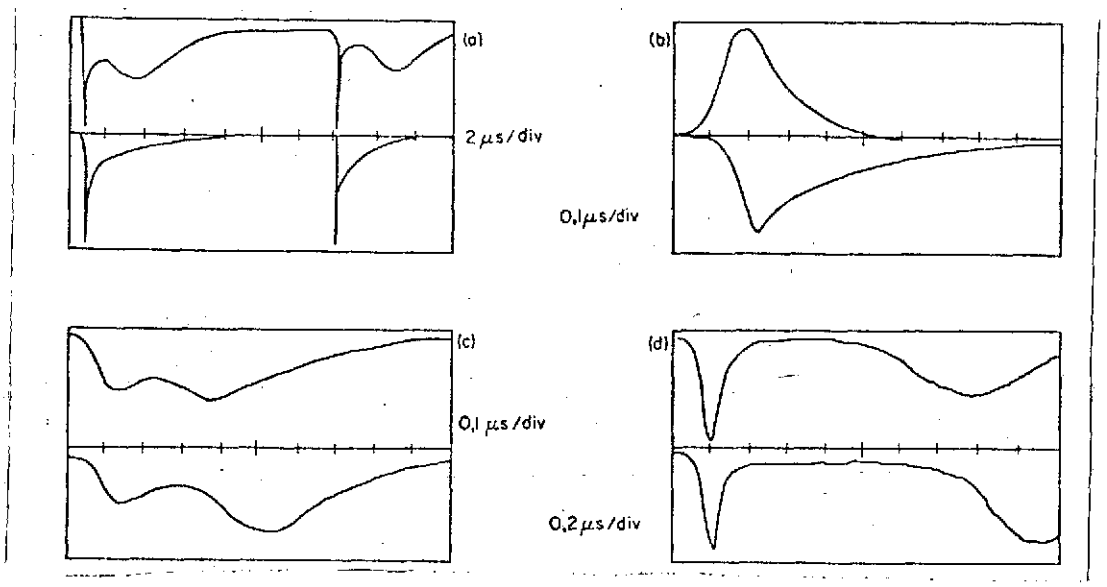

Fig. 7. Emission of zinc plasmas generated by separate pulses; emission at various heights above specimen surface [(a) top = 0 mm, bottom = 1.6 mm; (b) top = laser pulse, bottom = 1.6 mm; (c) top = 2.5 mm, bottom = 4.1 mm; (d) top = 8 mm, bottom = 9.6 mm]. The ordinates represent relative intensities.

However, these measurements provide little real information, since, as the irradiation density during the pulse increases, higher values (about 10^5 cm/sec) were measured for the propagation velocity of "vaporization shocks."

More informative are measurements taken on plasmas generated by multiple giant pulses with an average irradiation density of $2 \cdot 10^8$ W/cm^2. Fig. 7 (a) shows the emission of a Zn plasma in air directly above the specimen surface (upper curve) and 1.6 mm above it (lower curve). The lower curve in Fig. 7 (b) is the same as in 7 (a), but with an enlarged time scale, while the upper

curve is the laser pulse. Fig. 7 (c) depicts the emission behavior of the plasma 2.5 mm (top) and 4.1 mm (bottom) above the specimen surface. Fig. 7 (d) shows the emission even further above the specimen surface (top: 8 mm, bottom: 9.6 mm).

These differences in emission behavior of the plasma at various heights above the specimen surface, i.e. in different stages of expansion, can be accounted for as follows: the first peak in each case is explained as intensive radiation emission (predominantly bremsstrahlung) during the absorption of radiation in the plasma. The second one (lower peak in Fig. 7 (a)) is interpreted as a standard-temperature-like maximum, but not in the way studied by Krempl [42], because under the present conditions, the particle density is determined not only by the ideal gas law and the Saha equation, but also, increasingly, by the plasma expansion. When the plasma expands in a vacuum, this standard maximum is absent precisely because of this preponderance of expansion over the emission behavior of a cooling thermal plasma so conspicuous at constant pressure. The first peaks in Figs. 7 (c) and (d) represents the emission of a plasma generated by a preceding laser pulse, while the second peak originates in the expansion of the plasma just generated. With multiple impulses, the propagation velocity of the plasma, and thus the kinetic energy of the plasma components, can be determined from this second peak and the time between it and the laser pulse. Since the hotter plasma just after vaporization can be viewed as thermal and expands accordingly, the kinetic energy can be equated with the thermal energy $\bar{E} = \frac{1}{2}m\bar{u}^2 = \frac{3}{2}kT$. Under the conditions given above ($W = 2 \cdot 10^8$ W/cm^2, laser energy 35 mWsec, duration of pulse (half-power width) $2 \cdot 10^{-7}$ sec), the measurements yielded values of 3.5 eV, i.e. about 40,000°K, which are roughly consistent with the results found by Chang and Birdsall [12]. Within the limits /116
of measuring accuracy, no dependence upon specimen material could be established. Travel time measurements using the first peak

were interpreted here as giving the propagation velocity of the ionization wave in the sense of the view of Raizer [27]. The values of about $5 \cdot 10^6$ cm/sec under the existing conditions appear to justify this interpretation. This is also true when they are considered in combination with the estimates from the heights of the sharp continuous-spectrum boundary in the non-time-resolved photographically recorded spectra (Section 5). Even in the expanded plasma, i.e. far above the surface of the specimen, emission is directly excited by the laser pulse (Fig. 7(c, d). Hence, the radiation is absorbed so that there must be sufficient numbers of free electrons. This shows that the recombination of the plasma is incomplete. This observation has also been made on plasmas flowing from nozzles[1], since the degree of ionization is "frozen" by the rapid expansion.

Even though these studies have suppressed many details, they still supply the following picture of laser-generated plasmas: because of the high particle densities during vaporization, the plasmas acquire thermal properties due to an initially nonthermal ionization mechanism, which, like discharge ionization, has a threshold character. The rapidly expanding plasma cools, but its electron density is higher than the thermal one, because of the incomplete recombination rate contingent on relaxation of the recombination mechanism.

Acknowledgements: We are indebted to our esteemed teacher Dean H. Krempl for his encouragement and promotion of this work and to the German Research Society for providing the funds.

[1] Private communication from Dr. Artman, DVL-Institute, Stuttgart.

REFERENCES

1. Brech, F., Int. Conf. Spectry, X, Washington, 1962.
2. Debras-Guedon, J. and Liodec, N., Compt. Rend. 257, 3336 (1963).
3. Runge, E.F., Minck, R.W. and Bryan, I.R., Spectrochim. Acta 20, 733 (1964).
4. Hagenah, W.D., Z. Angew. Math. Phys. 16, 130 (1965).
5. Rasberry, S.D., Scribner, B.F. and Margoshes, M., XIV Coll. Spectros. Int., Exeter, 1965.
6. Piepmeier, E.H., Dissertation, University of Illinois, 1966.
7. Hagenah, W.D., Laqua, K. and Masterson, K.D., XIV Coll. Spectrosc. Int., Debrecen, 1967.
8. Ready, J.F., J. Appl. Phys. 36, 462 (1965).
9. Harris, T.J., IBM J. 7, 342 (1963).
10. Honig, R.E., Appl. Phys. Lett. 3, 8 (1963).
11. Howe, J.A. and Molloy, T.V., J. Appl. Phys. 35, 2265 (1964).
12. Chang, T.Y. and Birdsall, C.K., Appl. Phys. Lett. 5, 171 (1964).
13. Neuman, F., Appl. Phys. Lett. 4, 167 (1964).
14. Ehler, A.W., J. Appl. Phys. 37, 4962 (1966).
15. Ready, J.F., Appl. Phys. Lett. 3, 11 (1963).
16. Linlor, W.I., Appl. Phys. Lett. 3, 210 (1963).
17. Namba, S., Kim, P.H. and Mitsuyama, A., J. Appl. Phys. 37, 3330 (1966).
18. Gregg, D.W. and Thomas, S.J., J. Appl. Phys. 37, 4313 (1966).
19. Gregg, D.W. and Thomas, S.J., J. Appl. Phys. 37, 2787 (1966).
20. Archbold, E., Harper, D.W. and Hughes, T.P., Brit. J. Appl. Phys. 15, 1321 (1964).
21. Archbold, E. and Hughes, T.P., Nature 204, 670 (1964).
22. Opower, H. and Press, H., Z. Naturforsch. 21a, 344 (1966).

23. Linlor, W.I., Phys. Rev. Lett. 12, 383 (1964).

24. Askaryan, G.A. and Moroz, E.M., Soviet Phys. JETP 16, 1638 (1963).

25. Dawson, J.M., Phys. Fluids 7, 981 (1964).

26. Zeldovich, Ya.B. and Raizer, Yu.P., Soviet Phys. JETP 20, 20, 772 (1965).

27. Raizer, Yu.P., Soviet Phys. JETP 21, 1009 (1965).

28. Basov, N.G. and Krokhin, O.N., Soviet Phys. JETP 19, 123 (1964).

29. Krokhin, O.N., Z. Angew. Math. Phys. 16, 123 (1965).

30. Engelhardt, A.G., Westinghouse Res. Rep. 63-128-113-R2.

31. Carslaw, H.S. and Jaeger, J.C., Conduction of Heat in Solids, Clarendon Press, 1959.

32. Landau, H.G., Q. Appl. Math. 8, ,81 (1950); Masters, J.T., J. Appl. Phys. 27, 477 (1965); Vogel, K. and Backlung, P., J. Appl. Phys. 36, 3697 (1965).

33. Ready, J.F., Phys. Rev. 137A, 620 (1965).

34. Honig, R.E., RCA Rev. 23, 567 (1962).

35. Mentall, J.E. and Nicholls, R.W., J. Chem. Phys. 46, 2881 (1967).

36. Unsöld, A., Physik der Sternatmosphären [Physics of Stellar Atmospheres], Springer, 1955.

37. Röss, D., Laser Akademische [Laser Academic], 1966

38. Bögershausen, W. and Hönle, K., Spectrochim. Acta 24B, 71 (1969).

39. Glasstone, S. and Loveberg, R.H., Controlled Thermonuclear Reactions, Van Nostrand, 1960.

40. Bardocz, A., Vörös, T., and Vanyek, U.M., Z. Angew. Phys. 14, 581 (1962).

41. Griem, H.R., Plasma Spectroscopy, McGraw-Hill, 1964.

42. Krempl, H., Z. Phys. 167, 302 (1962).